



جامعة الملك عبد الله  
للعلوم والتقنية

King Abdullah University of  
Science and Technology

## Highly Efficient and Reproducible Nonfullerene Solar Cells from Hydrocarbon Solvents

Item Type	Article
Authors	Wadsworth, Andrew; Ashraf, Raja; Abdelsamie, Maged; Pont, Sebastian; Little, Mark S.; Moser, Maximilian; Hamid, Zeinab; Neophytou, Marios; Zhang, Weimin; Amassian, Aram; Durrant, James R.; Baran, Derya; McCulloch, Iain
Citation	Wadsworth A, Ashraf RS, Abdelsamie M, Pont S, Little M, et al. (2017) Highly Efficient and Reproducible Nonfullerene Solar Cells from Hydrocarbon Solvents. ACS Energy Letters: 1494–1500. Available: <a href="http://dx.doi.org/10.1021/acsendergylett.7b00390">http://dx.doi.org/10.1021/acsendergylett.7b00390</a> .
Eprint version	Post-print
DOI	<a href="https://doi.org/10.1021/acsendergylett.7b00390">10.1021/acsendergylett.7b00390</a>
Publisher	American Chemical Society (ACS)
Journal	ACS Energy Letters
Rights	This document is the Accepted Manuscript version of a Published Work that appeared in final form in ACS Energy Letters, copyright © American Chemical Society after peer review and technical editing by the publisher. To access the final edited and published work see <a href="http://pubs.acs.org/doi/abs/10.1021/acsendergylett.7b00390">http://pubs.acs.org/doi/abs/10.1021/acsendergylett.7b00390</a> .
Download date	04/08/2022 17:26:15
Link to Item	<a href="http://hdl.handle.net/10754/625072">http://hdl.handle.net/10754/625072</a>

# Highly Efficient and Reproducible Non-Fullerene Solar Cells from Hydrocarbon Solvents

*Andrew Wadsworth,<sup>\*†</sup> Raja S. Ashraf,<sup>‡</sup> Maged Abdelsamie,<sup>‡</sup> Sebastian Pont,<sup>†</sup> Mark Little,<sup>†</sup>  
Maximilian Moser,<sup>†</sup> Zeinab Hamid,<sup>†</sup> Marios Neophytou,<sup>‡</sup> Weimin Zhang,<sup>‡</sup> Aram Amassian<sup>‡</sup>  
James R. Durrant,<sup>†,§</sup> Derya Baran,<sup>‡</sup> and Iain McCulloch.<sup>†,‡</sup>*

<sup>†</sup>Department of Chemistry and Centre for Plastic Electronics, Imperial College London, London, SW7 2AZ, UK.

<sup>‡</sup>Physical Sciences and Engineering Division, KAUST Solar Center (KSC), King Abdullah University of Science and Technology (KAUST), KSC Thuwal 23955-6900, Saudi Arabia.

<sup>§</sup>SPECIFIC IKC, Swansea University, Baglan Bay Innovation Centre, Port Talbot, Swansea SA12 7AX, UK.

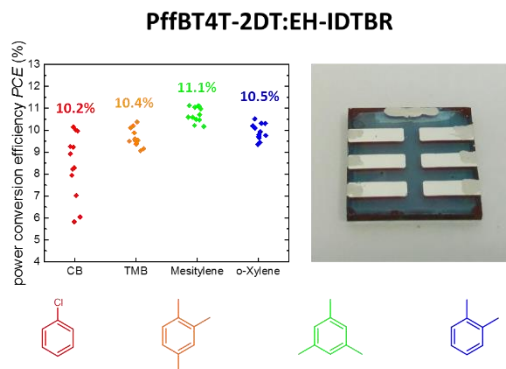
AUTHOR INFORMATION

**Corresponding Author**

[andrew.wadsworth11@imperial.ac.uk](mailto:andrew.wadsworth11@imperial.ac.uk)

## ABSTRACT

With chlorinated solvents unlikely to be permitted for use in solution-processed organic solar cells in industry, there must be a focus on developing non-chlorinated solvent systems. Here we report high efficiency devices utilising a low-bandgap donor polymer (PffBT4T-2DT) and a non-fullerene acceptor (EH-IDTBR), from hydrocarbon solvents and without using additives. When mesitylene was used as the solvent, rather than chlorobenzene, an improved power conversion efficiency (11.1%) was achieved without the need for pre- or post- treatments. Despite altering the processing conditions to environmentally friendly solvents and room temperature coating, grazing incident X-ray measurements confirmed that active layers processed from hydrocarbon solvents retained the robust nano-morphology obtained with hot-processed chlorinated solvents. The main advantages of hydrocarbon solvent processed devices, besides the improved efficiencies, were the reproducibility and storage lifetime of devices. Mesitylene devices showed better reproducibility and shelf-life up to 4000h with PCE dropping by only 8% of its initial value.



Whilst solution-processed organic photovoltaics offer the potential advantages of low cost and the opportunity of large scale production with roll-to-roll coating and printing techniques,<sup>1-4</sup> the prevalent use of chlorinated solvents to process devices is one of the factors that has limited their commercialisation and environmental sustainability. To date, almost all high performance organic solar cells (OSCs) are processed from chlorinated solvents, such as chlorobenzene (CB), o-dichlorobenzene (o-DCB) and chloroform (CF), owing to their ability to dissolve the highly planar low-bandgap donor polymers often utilised in OSCs, and their excellent film forming properties. Additionally, halogenated additives, such as 1,8-diiodooctane (DIO) and 1-chloronaphthalene (CN), are often used in high performance organic photovoltaics to prevent excessive vitrification and improve the blend morphology in the active layer of devices and thus the power conversion efficiency (PCE) that can be achieved.<sup>5-9</sup> The main drawbacks of such solvents and additives are that they pose significant risks to both humans and the environment,<sup>10</sup> as well as recent evidence that they can contribute to device instability.<sup>11</sup> Consequently, it has become clear that the replacement of chlorinated solvents with relatively benign hydrocarbon alternatives is an important step towards producing industrially viable and environmentally friendly OSCs. Whilst chlorinated solvents are used almost exclusively in active layer processing, the origin of their use is not fundamental, but is rather the result of the literature precedent that has been set over the last decade. There are aromatic non-chlorinated solvents that possess similar solubility and film forming properties to solvents such as CB, which should also be explored as processing solvents in the fabrication of OSCs. In addition to the ability to dissolve conjugated polymers, good solvents for processing OSCs tend to have reasonably high boiling points, such that they dry slowly as this improves the blend morphology.<sup>12-14</sup> However, slow drying leads to longer

residence times during fabrication, reducing the throughput of devices, hence a compromise must be reached.

Most attempts to process cells from non-chlorinated solvents have thus far yielded relatively low efficiencies in comparison to their chlorinated solvent processed counterparts.<sup>15-19</sup> This can be attributed to the poorer solubility of many conjugated donor polymers and fullerene acceptors in aromatic non-chlorinated solvents such as toluene and o-xylene. This leads to the formation of large domains and micrometer sized particles in the bulk heterojunction.<sup>15</sup> Recently, high efficiency (> 10%) fullerene based (PffBT4T-C<sub>9</sub>C<sub>13</sub>:PC<sub>70</sub>BM) devices, were processed from a fully hydrocarbon solvent system; 1,2,4-trimethylbenzene (TMB) with 2.5% 1-phenylnaphthalene (PN) as an additive.<sup>20</sup> Whilst these results are promising, the need to pre-heat the solutions and substrates to 100 °C in the reported system is detrimental for large scale fabrication of OSCs due to lack of reproducibility in the device performances. Additionally, the active layers must be held under vacuum to remove the high-boiling PN additive. Avoiding such treatment steps is important in the development of large scale OSC fabrication. The extensive use of heating in the fabrication of device active layers also presents issues for OSCs. The donor/acceptor blend is often deposited from hot solutions, and in some cases heated substrates, in order to obtain the optimum blend morphology. Thermal annealing is used frequently to optimise the blend morphology further, usually at temperatures over 120 °C. These high temperatures, particularly during annealing, are incompatible with most polyethylene terephthalate (PET) substrates,<sup>21</sup> which are commonly used to achieve flexible OSC modules. Therefore, if the processing conditions are too harsh for PET substrates, flexible modules cannot be produced and one of the key advantages that OSCs possess over silicon and other inorganic photovoltaics is lost. Additionally, an annealing step increases the residence time during the

fabrication process, thus avoiding such a step allows a higher throughput of devices, making for a more efficient manufacturing process.

Non-fullerene acceptors (NFAs) were initially developed to overcome the drawbacks associated with (phenyl-C<sub>60</sub>-butyric acid methyl ester) PC<sub>60</sub>BM and its derivatives; such as poor absorption in the visible region of the solar spectrum,<sup>22</sup> morphological instability in the active layer,<sup>23</sup> and the high cost associated with production of fullerenes.<sup>24</sup> Recent developments in non-fullerene acceptors, particularly perylene-diimide and acceptor-donor-acceptor (A-D-A) type molecules, have shown considerable promise and many can now match the performance achieved with fullerene acceptors for a number of polymers.<sup>8,25-30</sup> As such, non-fullerene acceptors can be considered as a competitive alternative to fullerenes in terms of device performance; it is therefore important to also develop non-chlorinated processing conditions that work well in these fullerene-free OSCs.

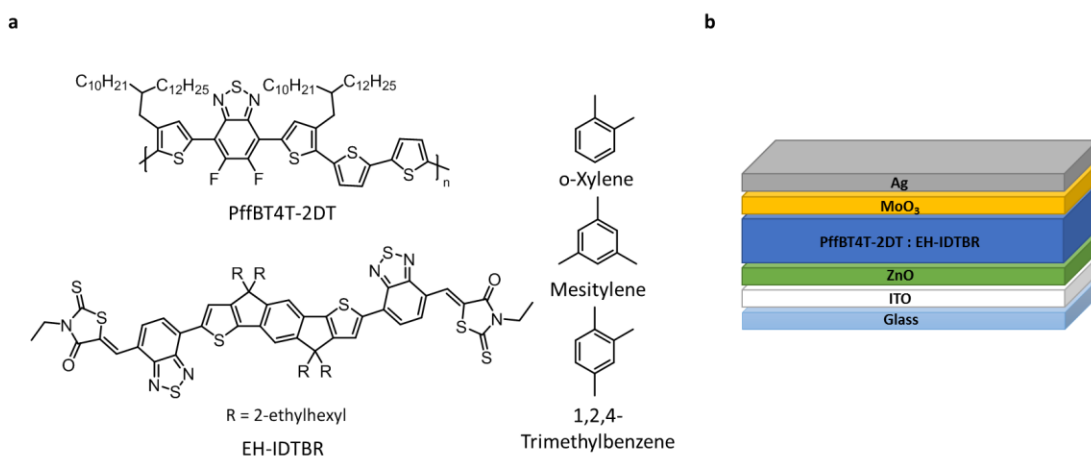


Figure 1. (a) Structures of PffBT4T-2DT, EH-IDTBR and the non-chlorinated solvents. (b) Schematic of the inverted device architecture of the devices fabricated in this study.

Bulk heterojunction OSCs were fabricated using poly[(5,6-difluoro-2,1,3-benzothiazol-4,7-diyl)-alt-(3,3''-di(2-decyltetradecyl)-2,2';5',2'';5''',2''''-quaterthiophen-5,5''''-diyl)] (PffBT4T-2DT) as the donor polymer; this has been previously reported to achieve 10.3% in fullerene containing devices when processed from the TMB-PN solvent system.<sup>20</sup> EH-IDTBR, a non-fullerene acceptor, had been previously reported to achieve 6.4% with P3HT,<sup>25</sup> but here this NFA has been combined with a low bandgap high performance donor polymer. An inverted architecture (ITO/ZnO/PffBT4T-2DT:EH-IDTBR/MoO<sub>3</sub>/Ag) was adopted and the active layer blends were processed from CB and a number of non-chlorinated solvents (1,2,4-trimethylbenzene, mesitylene and o-xylene), summarized in Fig. 1. An inverted architecture was chosen based upon the success that EH-IDTBR had previously displayed in inverted architecture OSCs,<sup>25</sup> and the excellent air stability that has previously been reported in inverted devices.<sup>31</sup>

The polymer/acceptor blend exhibited excellent solubility in each of the non-chlorinated solvents and a low viscosity solution could be prepared at reasonably low temperatures 40-60 °C, however elevated temperatures of 90-100 °C were needed to prepare a low viscosity solution from CB. At room temperature, the CB solution was observed to be extremely viscous in comparison to those prepared using the non-chlorinated solvents (see supplementary figure S1). A result of this apparent high viscosity solution in CB was poor homogeneity and large defects in films (see supplementary figure S1) that had been processed at ambient temperatures and with unheated substrates, therefore solution and substrate heating was required in order to achieve working devices. The ability to maintain constant substrate and solution temperatures is not particularly straightforward when spin-coating, suggesting that reproducibility may be an issue for the CB processed devices. In contrast, the lower viscosity solutions from the non-chlorinated

solvents allowed for uniform and homogeneous films to be deposited at ambient temperatures and with greater repeatability.

Table 1. J-V Characteristics of the inverted structure PffBT4T-2DT:EH-IDTBR devices.

<b>processing solvent</b>	<b>V<sub>OC</sub> (V)</b>	<b>J<sub>SC</sub> (mA cm<sup>-2</sup>)</b>	<b>FF</b>	<b>max PCE/ average PCE<sup>a</sup> (%)</b>	<b>standard deviation<sup>a</sup></b>	<b>average thickness<sup>a</sup> (nm)</b>
<b>CB</b>	<b>1.05</b>	<b>15.4</b>	<b>0.62</b>	<b>10.2 / 8.4</b>	<b>1.48</b>	<b>100</b>
<b>TMB</b>	<b>1.01</b>	<b>16.9</b>	<b>0.61</b>	<b>10.4 / 9.7</b>	<b>0.41</b>	<b>85</b>
<b>Mesitylene</b>	<b>1.02</b>	<b>17.2</b>	<b>0.63</b>	<b>11.1 / 10.7</b>	<b>0.35</b>	<b>80</b>
<b>o-Xylene</b>	<b>1.01</b>	<b>16.3</b>	<b>0.64</b>	<b>10.5 / 9.9</b>	<b>0.37</b>	<b>85</b>

Devices were measured under standard AM1.5G illumination at 100 mW cm<sup>-2</sup>, V<sub>OC</sub> is the open circuit voltage, J<sub>SC</sub> is the short circuit current, FF is the fill factor and PCE is the power conversion efficiency. (a) Average PCE, standard deviation and average thickness were calculated over 12 devices.

From the J-V characteristics (see Table 1 and Fig. 2a) it is clear that the devices processed from non-chlorinated solvents were able to exceed the PCE of devices processed from CB, with the best mesitylene device achieving 11.1%. Despite the slight drop in V<sub>OC</sub> observed, by 30 - 40 mV, the higher PCE obtained from the non-chlorinated processing solvents can be mainly attributed to a slight improvement in the J<sub>SC</sub>. In particular, the mesitylene processed devices were able to achieve a J<sub>SC</sub> of almost 2 mA cm<sup>-2</sup> greater than the CB processed device, despite being around 20 nm thinner. The increased absorption coefficient of the blend processed from mesitylene (see supplementary figure S2) can be used to suggest the origin of the improved J<sub>SC</sub>. Per unit thickness, the mesitylene processed blend is able to absorb a greater fraction of incident photons than the CB blend, and thus a greater photocurrent could be achieved. The thicker active layers obtained when devices were processed from CB are likely to be a result of the higher



viscosity of this solution, in comparison to those prepared from non-chlorinated solvents. The higher viscosity would lead to poorer spreading of the solution on the surface of the substrate, thereby producing thicker films.

Contrary to many of the most successful non-chlorinated solvent systems reported to date,<sup>20,28,32,33</sup> a high boiling point additive did not improve the device performance in the case of this system. Using the aforementioned TMB:PN (97.5:2.5) solvent system,<sup>20</sup> PffBT4T-2DT:EH-IDTBR devices were in fact worse than using only TMB for processing (see supplementary table S1). This is likely to be because the PN additive usually aids in solubilising the fullerene acceptors in the active layer blend; this is not necessary due to the use of a non-fullerene acceptor in the active layer blend; this is not necessary due to the use of a non-fullerene acceptor with improved solubility, and instead the additive is likely to have led to greater phase separation in the blend.

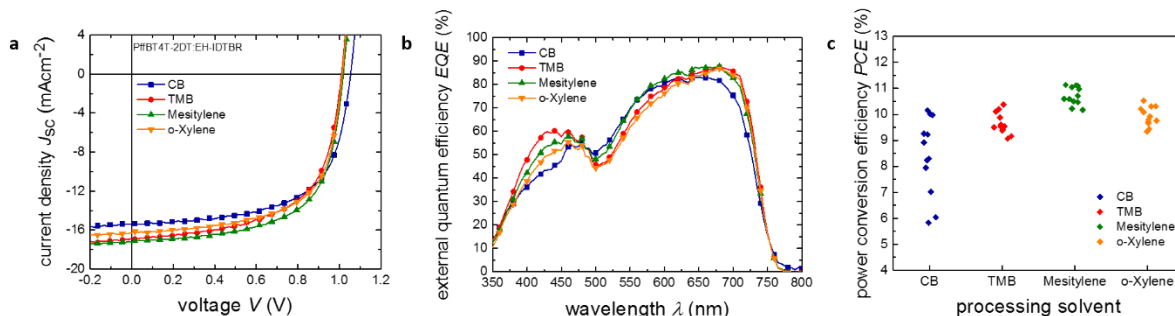


Figure 2. (a) J-V characteristic curves of the inverted structure PffBT4T-2DT:EH-IDTBR devices. (b) EQE of the same devices. (c) Distribution in PCE of 12 devices processed from each solvent.

The external quantum efficiency (EQE) shown in Fig. 2 is not particularly broad in these devices, with a large fraction of the exciton generation occurring between 500 – 750 nm; however the EQE<sub>max</sub> for these devices is exceptionally high (83% for the CB device, 87% for each of the non-chlorinated solvent processed devices). The most likely reason for this is the

cumulative donor and acceptor absorption in the 500-750 nm region of the solar spectrum, since the absorption profiles of the donor and acceptor materials are very similar (see supplementary figure S3a). It should be noted that the wavelength ( $\lambda_{\text{max}}$ ) corresponding to  $\text{EQE}_{\text{max}}$  differs slightly between the CB and mesitylene processed devices, with an approximate 30 nm bathochromic shift when the devices are processed from the non-chlorinated solvents. This may be indicative of small structural differences in the active layer blend, where increasing aggregation leads to a red shift in absorption and a similar trend can be seen in the thin film absorption spectra of the active layer blends from the various solvents (see supplementary figure S3b).

In addition to the slight improvement in performance for devices processed from the non-chlorinated solvents, another obvious advantage of using the non-chlorinated solvents for processing the active layer is the reproducibility of the devices. It is clear from Fig. 2c that devices processed from the non-chlorinated solvents, particularly mesitylene, show a small spread in PCEs achieved across 12 devices. However, the CB processed devices suffer from much poorer reproducibility, with a wider range of PCEs being obtained. This can be quantified by calculating the standard deviation of each set of devices (see Table 1). The standard deviation of the set of CB processed devices is over 4 times larger than that of the set of mesitylene processed devices, indicating a large disparity in reproducibility between the CB and mesitylene processing conditions. As eluded to above, the likely reason for the improved reproducibility of the devices processed from non-chlorinated solvents is the fact that active layers can be processed from a low viscosity solution at relatively low temperatures, whereas a temperature of at least 100 °C was needed for both the solution and the substrates when processing from CB. Since it is difficult to maintain solution and substrate temperatures during spin-coating, it is

likely that the active layer solutions were cooling at different rates during spin-coating for each CB processed device. Variable cooling rates would lead to less control over aggregation and viscosity of the solution during deposition, thereby yielding inhomogeneity and a range of thickness in the thin films, and thus poorer reproducibility.

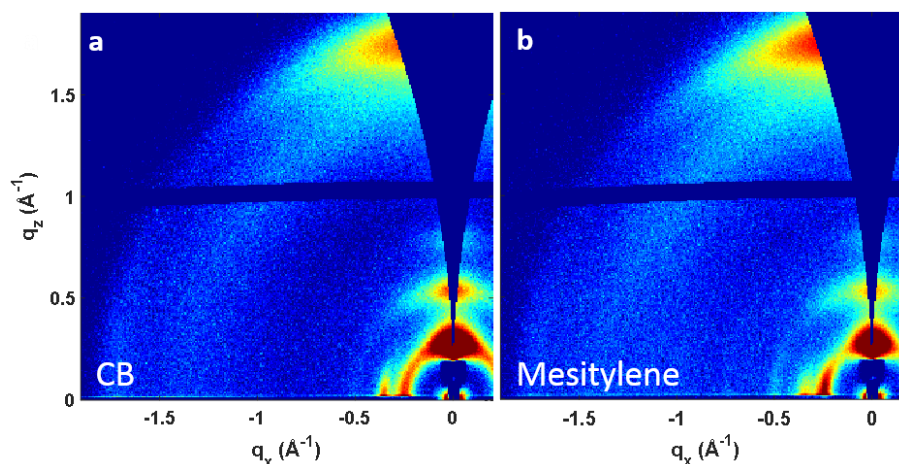


Figure 3. Two-dimensional GIWAXS images of the PffBT4T-2DT:EH-IDTBR (1:1) active layers processed from (a) CB and (b) Mesitylene

Previous studies on PffBT4T-2DT in OSCs attribute its success, in part, to the temperature-dependent aggregation effects of the polymer in a CB solution.<sup>20,34,35</sup> Temperature-dependent UV-Vis absorption spectra were also taken in mesitylene (see supplementary information supplementary figure S4) and identical aggregation behaviour was observed to that previously reported for a solution in CB.<sup>34</sup> Deaggregation became obvious above 60 °C and the solution appeared to become fully deaggregated at 90-100 °C. Since the CB and non-chlorinated active layers were processed at different temperatures, the morphological characteristics of the blends were probed to investigate whether this led to structural differences by altering aggregation in the films as they formed. Grazing incidence wide angle x-ray scattering (GIWAXS) analysis of the

PffBT4T-2DT:EH-IDTBR blends showed that for both CB and mesitylene processed films the donor polymer displayed a high degree of order indicated by multiple diffraction peaks (h00), these polymer crystallites exhibit dominant face-on orientation as revealed by the dominant  $\pi$ -stacking scattering in the out-of-plane direction (see Fig. 3 and supplementary figure S5). It must be noted that these films were relatively thick compared to the device active layers ( $\sim 400$  nm), however both films were very similar in thickness such that a comparison between the films could be made. The two blends showed similar morphological features for the most part, despite the different processing solvent and temperature. Diffraction peaks for both lamellar and  $\pi$ -stacking of the polymer were present and whilst acceptor scattering was obvious in the in-plane direction (see supplementary figure S6), the mesitylene processed blend did have slightly lower relative crystallinity of the polymer lamellar stacking in comparison to the CB processed blend, but the  $\pi$ -stacking was unaffected. The small improvement in the relative crystallinity of the polymer lamellar stacking in the CB processed active layer is likely to be facilitated by processing from a hot solution and substrate where there is less aggregation in the initial solution prior to deposition. However, the mesitylene processed blend has more in-plane contribution to the polymer lamellar stacking, which contributes to the crystallites with face-on orientation, which thereby explains the fact that the overall  $\pi$ -stacking scattering was unaffected by the reduction of lamellar stacking as compared to the CB blend (see line-cuts of the in-plane and out-of-plane scattering in supplementary figure S6).<sup>36</sup>

In addition to the environmental and safety issues associated with the use of chlorinated solvents and additives in device processing, it has also been suggested that the use of halogenated additives such as DIO and CN can negatively impact upon the photo-stability of devices.<sup>11</sup> However, the morphological stability of devices can be strongly influenced by the

solvent used, in addition to additives.<sup>37,38</sup> With high efficiency devices being demonstrated routinely, the focus for viable OSC technology should now be on producing highly stable devices too. The storage lifetime and photo-stability of the CB and mesitylene processed devices, under an inert atmosphere, were probed in order to investigate the role of the processing solvent on device stability.

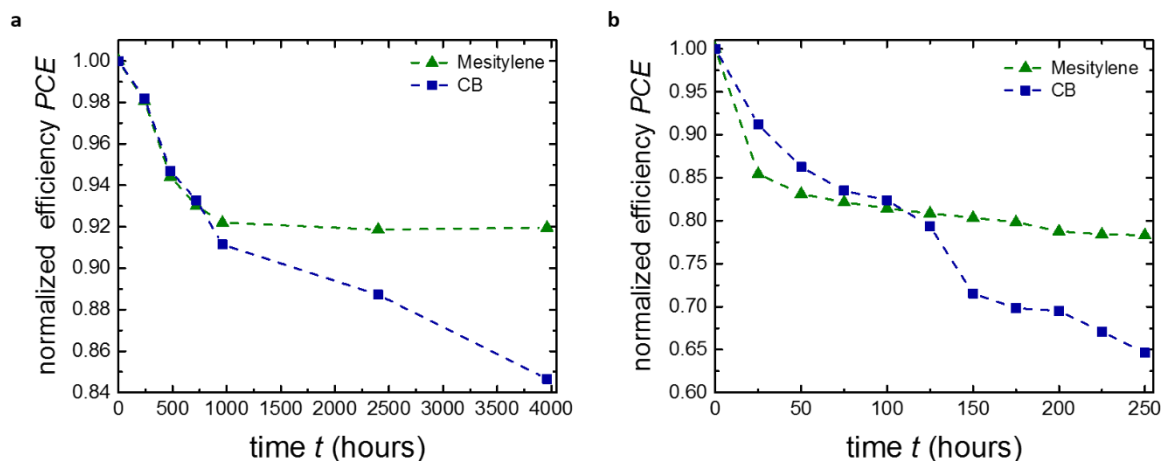


Figure 4. (a) Storage lifetime study for optimized PffBT4T-2DT:EH-IDTBR cells from CB and mesitylene stored in the dark under  $N_2$  over a period of 4000 hours. (b) Photo-stability of optimized PffBT4T-2DT:EH-IDTBR cells from CB and mesitylene kept under  $N_2$  and constant white light illumination for 250 hours, where J-V characteristics were measured every 25 hours.

To assess the storage lifetime, unencapsulated devices were kept in an inert atmosphere, in the dark, and the J-V characteristics were measured periodically over the course of 4000 hours. It is clear from Fig. 4 that devices processed from both CB and mesitylene display relatively impressive storage lifetime, with both devices retaining approximately 92% of their initial PCE over the course of 1000 hours. After 2400 hours the mesitylene processed device still possessed 92% of its initial PCE, however the CB processed device's PCE had continued to drop to 88% of its initial value. A final measurement at 4000 hours confirmed that the mesitylene devices had

stabilized as it was still able to achieve 92% of its initial PCE, however the CB processed device had continued to degrade, by 4000 hours achieving 84% of its initial PCE. A possible reason for the discrepancy in stability between the CB and mesitylene processed devices is a result of differences in the long-term morphological stability of the devices. The CB processed blend appears to phase separate over extended periods of time, whereas small phase separated crystallites appeared to form in the mesitylene processed devices (see supplementary figures S7 and S8). The phase separation in the CB blend occurs on the micrometer scale, far larger than the exciton diffusion length, hence exciton relaxation and recombination is likely to lead to a reduced photocurrent over time.

To probe the photo-stability, the J-V characteristics of CB and mesitylene processed devices, kept under constant illumination with white light, were measured incrementally over the course of 10 days. As Fig. 4b shows, the device processed from mesitylene appears to be more stable than the device processed from CB under illumination. The PCE of the mesitylene device drops to 78% of its initial value over 10 days, whereas the PCE of the CB device drops to 65% of its initial value, over the 10 day period. The initial drop in the PCE of the mesitylene device, often referred to as a burn-in,<sup>39</sup> can be attributed to a sharp decrease in  $V_{OC}$  during the first day of illumination, however the device retained over 97% of the initial  $J_{SC}$  and FF during the same period (see supplementary figures S9-S11). Following the burn in period, a small drop in the  $J_{SC}$  (6%) can be seen over the subsequent 9 days, but in general the device's performance stabilizes considerably. A similar burn in was also observed in the CB device, however the initial drop in  $V_{OC}$  was accompanied with a steady drop in  $J_{SC}$  across the 10 day period (24% loss) whilst the FF remained relatively constant throughout the measurements (see supplementary figures S9-

S11). This larger decrease in  $J_{SC}$  observed in the CB processed device accounts for the greater loss in overall PCE, in comparison to the mesitylene processed device.

The UV-Vis absorption spectra of the PffBT4T-2DT:EH-IDTBR blends before and after UV and white light photo-bleaching in an inert atmosphere showed no change in features or intensity; indicating that photo-bleaching of the active layer was not occurring (see supplementary figures S12 and S13). Therefore, the drop in PCE is unlikely to be a result of photo-degradation of PffBT4T-2DT and EH-IDTBR. There have been reports that photo-degradation of the ZnO electron transport layer is responsible for a drop in  $V_{OC}$  in inverted OSCs when; this may explain the initial drop in  $V_{OC}$  observed in both the CB and mesitylene processed devices.<sup>40,41</sup> It must be noted that the operational device stability data is preliminary work, and at this stage confirms that a non-chlorinated solvent device can at least match the operating stability of its chlorinated solvent processed counterpart. However, due to the complexity of degradation mechanisms in OSCs further studies must be carried out to fully explain the origin and extent to which the operational stabilities differ between devices processed from chlorinated and non-chlorinated solvents.

In conclusion, the replacement of CB with mesitylene led to an improvement in device PCE from 10.2 to 11.1%. The improvements achieved in the mesitylene devices can be attributed to a greater  $J_{SC}$  despite the reduced thickness of the active layer. In addition to the small improvement in PCE when the non-chlorinated processing solvent was used, an improvement in the reproducibility of devices is also seen. The high viscosity solution from CB at ambient conditions meant that hot processing conditions were necessary, however the inability to closely control the temperature during the spin-coating is likely to have led to the differences in thickness and morphology between devices, and thus poorer reproducibility. GIWAXS indicated

that despite the different processing conditions, the morphology of the blends was reasonably similar. In all cases the face-on orientation dominated and a high degree of order was observed for the polymer. Better storage stability was seen in the mesitylene processed devices, which can be attributed to improved long-term morphological stability of the blends from mesitylene, relative to CB. This was confirmed by the micrometer scale phase separation that was seen in the DF-TEM images of films aged for 150 days in the CB active layer, whereas much smaller crystallites were present in the mesitylene active layer blend. An initial study into the operational stability of devices suggested that devices processed from mesitylene are at least as stable, and possibly more stable than, CB processed devices. Further investigation is needed to determine the origin and extent of the improved stability in mesitylene processed devices. In addition to the improved photovoltaic performance and stability exhibited in the mesitylene processed devices, the fact that they do not require the use of chlorinated solvents or additives during fabrication is hugely advantageous. The reduced risk of harm to both humans and the environment from the hydrocarbon solvents, along with the introduction of more ambient processing conditions, leaves this system more industrially viable than many of the state-of-the-art organic solar cell system reported. Overall, this is a promising system that makes use of an environmentally friendly processing solvent and can produce PCEs among the best for organic solar cells in a facile and reproducible way.

## ASSOCIATED CONTENT

### **Supporting Information.**

Experimental procedure for device fabrication, characterization and stability studies, along with supplementary figures and tables. Images of the active layer blends, device data for additive



containing devices, UV-vis absorption spectra of neat materials and blends, additional GIWAXS data, DF-TEM images of the active layers, additional stability data and UV-vis absorption spectra from photo-bleaching experiments.

#### AUTHOR INFORMATION

**Email:** [andrew.wadsworth11@imperial.ac.uk](mailto:andrew.wadsworth11@imperial.ac.uk)

**ORCID:** 0000-0002-9050-0599

#### Notes

The authors declare no competing financial interest.

#### ACKNOWLEDGMENT

The authors thank KAUST for financial support, the Welsh Assembly Government Sêr Solar Project and acknowledge EC FP7 Project SC2 (610115), EC H2020 (643791), and EPSRC Projects EP/G037515/1, EP/M005143/1, EP/L016702/1.

#### REFERENCES

- (1) Li, G.; Zhu, R.; Yang, Y. Polymer Solar Cells. *Nat. Photonics*, **2012**, *6*, 153-161
- (2) Søndergaard, R. R.; Hösel, M.; Krebs, F. C. Roll-to-Roll Fabrication of Large Area Functional Organic Materials. *J. Polym. Sci. B. Polym. Phys.* **2012**, *51*, 16-34
- (3) Galagan, Y.; de Vries, I. G.; Langen, A. P.; Andriessen, R.; Verhees, W. J. H.; Veenstra, S. C.; Kroon, J. M. Technology Development for Roll-to-Roll Production of Organic Photovoltaics. *Chem. Eng. Process.* **2011**, *50*, 454-461

(4) Eggenhuisen, T. M.; Galagan, Y.; Biezmens, A. F. K. V.; Slaats, T. M. W. L.; Voorthuizen, W. P.; Kommeren, S.; Shanmugam, S.; Teunissen, J. P.; Hadipour, A.; Verhees, W. J. H. et al. High Efficiency, Fully Inkjet Printed Organic Solar Cells with Freedom of Design. *J. Mater. Chem. A*, **2015**, *3*, 7255-7262

(5) Choi, H.; Ko, S. J.; Kim, T.; Morin, P. O.; Walker, B.; Lee, B. H.; Leclerc, M.; Kim, J. Y.; Heeger, A. J. Small Bandgap Polymer Solar Cells with Unprecedented Short Circuit Current Density and High Fill Factor. *Adv. Mater.* **2015**, *27*, 3318-3325

(6) He, Z.; Xiao, B.; Liu, F.; Yang, Y.; Xiao, S.; Wang, C.; Russell, T. P.; Cao, Y. Single-Junction Polymer Solar Cells with High Efficiency and Photovoltage. *Nat. Photonics*, **2015**, *9*, 174-179

(7) Huo, L.; Liu, T.; Sun, X.; Cai, Y.; Heeger, A. J.; Sun, Y. Single-Junction Organic Solar Cells Based on a Novel Wide-Bandgap Donor Polymer with Efficiency of 9.7%. *Adv. Mater.* **2015**, *27*, 2938-2944

(8) Zhao, W.; Qian, D.; Zhang, S.; Li, S.; Inganäs, O.; Gao, F.; Hou, J. Fullerene-Free Polymer Solar Cells with Over 11% Efficiency and Excellent Thermal Stability. *Adv. Mater.* **2016**, *28*, 4734-4739

(9) Abdelsamie, M.; Treat, N. D.; Zhao, K.; McDowell, C.; Burgers, M. A.; Li, R.; Smilgies, D. M.; Stingelin, N.; Bazan, G. C.; Amassian, A. Toward Additive-Free Small-Molecule Organic Solar Cells: Roles of the Donor Crystallization Pathway and Dynamics. *Adv. Mater.* **2015**, *27*, 7285-7292

(10) Anderson, T. R.; Larsen-Olsen, T. T.; Andreasen, B.; Böttiger, A. P. L.; Carlé, J. E.; Helgesen, M.; Bundgaard, E.; Norrman, K.; Andreasen, J. W.; Jørgensen, M. et al. Aqueous Processing of Low-Band-Gap Polymer Solar Cells Using Roll-to-Roll Methods. *ACS Nano*. **2011**, *5*, 4188-4196

(11) Tremolet de Villers, B. J.; O'Hara, K. A.; Ostrowski, D. P.; Biddle, P. H.; Shaheen, S. E.; Chabynyc, M. L.; Olson, D. C.; Kopidakis, N. Removal of Residual Diiodooctane Improves Photostability of High-Performance Organic Solar Cell Polymers. *Chem. Mater.* **2016**, *28*, 876-884

(12) Li, G.; Shrotriya, V.; Huang, J.; Yao, Y.; Moriarty, T.; Emery, K.; Yang, Y. High-Efficiency Solution Processable Polymer Photovoltaic Cells by Self-Organization of Polymer Blends. *Nat. Mater.* **2005**, *4*, 864-868

(13) Schmidt-Hansberg, B.; Sanyal, M.; Klein, M. F. G.; Pfaff, M.; Schnabel, N.; Jaiser, S.; Vorobiev, A.; Müller, E.; Colsmann, A.; Scharfer, P. et al. Moving Through the Phase Diagram: Morphology Formation in Solution Cast Polymer-Fullerene Blend Films for Organic Solar Cells. *ACS Nano*, **2011**, *5*, 8579-8590

(14) Abdelsamie, M.; Zhao, K.; Niazi, M. R.; Chous, K. W.; Amassian, A. In Situ UV-Visible Absorption During Spin-Coating of Organic Semiconductors: A New Probe for Organic Electronics and Photovoltaics. *J. Mater. Chem. C*, **2014**, *2*, 3373-3381

(15) Shaheen, S. E.; Brabec, C. J.; Sariciftci, N. S.; Padinger, F.; Fromherz, T.; Hummelen, J. C. 2.5% Efficient Organic Plastic Solar Cells. *Appl. Phys. Lett.* **2001**, *78*, 841

(16) Schmidt-Hansberg, B.; Sanyal, M.; Grossiord, N.; Galagan, Y.; Baunach, M.; Klein, M. F. G.; Colsmann, A.; Scharfer, P.; Lemmer, U.; Dosch, H. et al. Investigation of Non-Halogenated Solvent Mixtures For High Throughput Fabrication of Polymer-Fullerene Solar Cells. *Sol. Energy Mat. Sol. Cells*, **2012**, *96*, 195-201

(17) Chen, X.; Liu, X.; Burgers, M. A.; Huang, Y.; Bazan, G. C. Green-Solvent-Processed Molecular Solar Cells. *Angew. Chem. Int. Ed.* **2014**, *53*, 14378-14381

(18) Deng, Y.; Li, W.; Liu, L.; Tian, H.; Xie, Z.; Geng, Y.; Wang, F. Low Bandgap Conjugated Polymers Based on Mono-Fluorinated Isoindigo for Efficient Bulk Heterojunction Polymer Solar Cells Processed with Non-Chlorinated Solvents. *Energy Environ. Sci.* **2015**, *8*, 585-591

(19) Zhao, W. Ye, L.; Zhang, S.; Sun, M.; Hou, J. A Universal Halogen-Free Solvent System for Highly Efficient Polymer Solar Cells. *J. Mater. Chem. A*, **2015**, *3*, 12723-12729

(20) Zhao, J.; Li, Y.; Yang, G.; Jiang, K.; Lin, H.; Ade, H.; Ma, W.; Yan, H. Efficient Organic Solar Cells Processed from Hydrocarbon Solvents. *Nat. Energy*, **2016**, *1*, 15027

(21) Jagadamma, L. K.; Abdelsamie, M.; El Labban, A.; Aresu, E.; Ngongang Ndjawa, G. O.; Anjum, D. H.; Cha, D.; Beaujuge, P. M.; Amassian, A. Efficient Inverted Bulk-Heterojunction Solar Cells from Low-Temperature Processing of Amorphous ZnO Buffer Layers. *J. Mater. Chem. A*, **2014**, *2*, 13321

(22) Lin, Y.; Zhan, X. Non-Fullerene Acceptors Organic Photovoltaics: An Emerging Horizon. *Mater. Horiz.* **2014**, *1*, 470-488

- (23) Dupont, S.; Oliver, M.; Krebs, F. C.; Dauskardt, R. Interlayer Adhesion in Roll-to-Roll Processed Flexible Inverted Polymer Solar Cells. *Sol. Energy Mat. Sol. Cells*, **2012**, *97*, 171-175
- (24) Mojica, M.; Alonso, J.; Mèndez, F. Synthesis of Fullerenes. *J. Phys. Org. Chem.* **2013**, *26*, 526-539
- (25) Holliday, S.; Ashraf, R. S.; Wadsworth, A.; Baran, D.; Yousaf, S. A.; Nielsen, C. B.; Tan, C. H.; Dimitrov, S. D.; Shang, Z.; Gasparini, N. et al. High-Efficiency and Air-Stable P3HT-Based Solar Cells with a New Non-Fullerene Acceptors. *Nat. Commun.* **2016**, *7*, 11585
- (26) Lin, Y.; He, Q.; Zhao, F.; Huo, L.; Mai, J.; Lu, X.; Su, C. J.; Li, T.; Wang, J.; Zhu, J. et al. A Facile Planar Fused-Ring Electron Acceptor for As-Cast Polymer Solar Cells with 8.71% Efficiency. *J. Am. Chem. Soc.* **2016**, *138*, 2973-2976
- (27) Meng, D.; Sun, D.; Zhong, C.; Liu, T.; Fan, B.; Huo, L.; Li, Y.; Jiang, W.; Choi, H.; Kim, T. et al. High-Performance Solution-Processed Non-Fullerene Organic Solar Cells Based on Selenophene-Containing Perylene Bisimide Acceptor. *J. Am. Chem. Soc.* **2016**, *138*, 375-380
- (28) Sprau, C.; Buss, F.; Wagner, M.; Landerer, D.; Koppitz, M.; Schulz, A.; Bahro, D.; Schabel, W.; Scharfer, P.; Colsmann, A. Highly Efficient Polymer Solar Cells Cast from Non-Halogenated Xylene/Anisaldehyde Solution. *Energy, Environ. Sci.* **2015**, *8*, 2744-2752
- (29) Baran, D.; Ashraf, R. S.; Hanifi, D. A.; Abdelsamie, M.; Gasparini, N.; Röhr, J. A.; Holliday, S.; Wadsworth, A.; Lockett, S.; Neophytou, M. et al. Reducing the Efficiency-Stability-Cost Gap of Organic Photovoltaics with Highly Efficient and Stable Small Molecule Acceptor Ternary Solar Cells. *Nat. Mater.* **2017**, *16*, 363-369

(30) Baran, D.; Kirchartz, T.; Wheeler, S.; Dimitrov, S. D.; Abdelsamie, M.; Gorman, J.; Ashraf, R. S.; Holliday, S.; Wadsworth, A.; Gasparini, N. et al. Reduced Voltage Losses Yield 10% Efficient Fullerene Free Organic Solar Cells with > 1V Open Circuit Voltages. *Energy Environ. Sci.* **2016**, *9*, 3783-3793

(31) Tan, M. J.; Zhong, S.; Li, J.; Chen, Z.; Chen, W. Air-Stable Efficient Inverted Polymer Solar Cells Using Solution-Processed Nanocrystalline ZnO Interfacial Layer, *ACS Appl. Mater. Interfaces*, **2013**, *5*, 4696–4701

(32) Park, C. D.; Fleetham, T. A.; Li, J.; Vogt, D. B. High Performance Bulk-Heterojunction Organic Solar Cells Fabricated with Non-Halogenated Solvent Processing. *Org. Electron.* **2011**, *12*, 1465-1470

(33) Cai, W.; Liu, P.; Jin, Y.; Xue, Q.; Russell, T. P.; Huang, F.; Yip, H. L.; Cao, Y. Morphology Evolution in High-Performance Polymer Solar Cells Processed from Nonhalogenated Solvents. *Adv. Sci.* **2015**, *2*, 1500095

(34) Chen, Z.; Cai, P.; Chen, J.; Liu, X.; Zhang, L.; Lan, L.; Peng, J.; Ma, Y.; Cao, Y. Low Band-Gap Conjugated Polymers with Strong Interchain Aggregation and Very High Hole Mobility Towards Highly Efficient Thick-Film Polymer Solar Cells. *Adv. Mater.* **2014**, *26*, 2586-2591

(35) Ro, H. W.; Downing, J. M.; Engmann, S.; Herzing, A. A.; DeLongchamp, D. M.; Richter, L. J.; Mukherjee, S.; Ade, H.; Abdelsamie, M.; Jagadamma, L. K. et al. Morphology Changes Upon Scaling a High-Efficiency, Solution Processed Solar Cell. *Energy Environ. Sci.* **2016**, *9*, 2835-2846

(36) Müller-Buschbaum, P. The Active Layer Morphology of Organic Solar Cells Probed with Grazing Incidence Scattering Techniques. *Adv. Mater.* **2014**, *26*, 7692-7709

(37) Ye, L.; Jiang, Y.; Guo, X.; Sun, H.; Zhang, S.; Zhang, M.; Huo, L.; Hou, J. Remove the Residual Additives Toward Enhanced Efficiency with High Reproducibility in Polymer Solar Cells. *J. Phys. Chem. C*, **2013**, *117*, 14920-14928

(38) Ciammaruchi, L.; Brunetti, F.; Visoly-Fisher, I. Solvent Effects on the Morphology and Stability of PTB7:PCBM Based Solar Cells. *Solar Energy*, **2016**, *137*, 490-499

(39) Heumueller, T.; Mateker, W. R.; Sachs-Quintana, I. T.; Vandewal, K.; Bartlet, J. A.; Burke, T. M.; Ameri, T.; Brabec, C. J.; McGehee, M. D. Reducing Burn-In Voltage Loss in Polymer Solar Cells By Increasing the Polymer Crystallinity. *Energy Environ. Sci.* **2014**, *7*, 2974-2980

(40) Kam, Z.; Wang, X.; Zhang, J.; Wu, J. Elimination of Burn-In Open Voltage Degradation By ZnO Surface Modification in Organic Solar Cells. *ACS Appl. Mater. Interfaces*, **2015**, *7*, 1608–1615

(41) Manor, A.; Katz, E. A.; Tromholtz, T.; Krebs, F. C. Electrical and Photo-Induced Degradation of ZnO Layers in Organic Photovoltaics. *Adv. Energy Mater.* **2011**, *1*, 836-843